

ENTRYWISE CONVERGENCE OF ITERATIVE METHODS FOR EIGENPROBLEMS

VASILEIOS CHARISOPOULOS* AUSTIN R. BENSON† ANIL DAMLE‡

June 21, 2022

Abstract

Several problems in machine learning, statistics, and other fields rely on computing eigenvectors. For large scale problems, the computation of these eigenvectors is typically performed via iterative schemes such as subspace iteration or Krylov methods. While there is classical and comprehensive analysis for subspace convergence guarantees with respect to the spectral norm, in many modern applications other notions of subspace distance are more appropriate. Recent theoretical work has focused on perturbations of subspaces measured in the $\ell_{2 \rightarrow \infty}$ norm, but does not consider the actual computation of eigenvectors. Here we address the convergence of subspace iteration when distances are measured in the $\ell_{2 \rightarrow \infty}$ norm and provide deterministic bounds. We complement our analysis with a practical stopping criterion and demonstrate its applicability via numerical experiments. Our results show that one can get comparable performance on downstream tasks while requiring fewer iterations, thereby saving substantial computational time.

1 Introduction & Background

Spectral methods play a fundamental role in machine learning, statistics, and data mining. Methods for foundational tasks such as clustering (Von Luxburg, 2007); semi-supervised learning (Mahoney et al., 2012); linear and nonlinear dimensionality reduction (Belkin and Niyogi, 2002; Friedman et al., 2001; Roweis and Saul, 2000); latent factor models (Gower, 2014) ranking and preference learning (Maystre and Grossglauser, 2015; Vigna, 2016); and covariance estimation all use information about eigenvalues and eigenvectors (or singular values and singular vectors) from an underlying data matrix. Often, spectral approaches outperform their “traditional” counterparts. For example, in spectral clustering applied to a point cloud, one forms a pairwise distance matrix, computes k eigenvectors of the associated graph Laplacian, and applies a method

*Department of Operations Research & Information Engineering, Cornell University, 14853 Ithaca, NY. Email: vc333@cornell.edu

†Department of Computer Science, Cornell University, 14853 Ithaca, NY. Email: arb@cs.cornell.edu

‡Department of Computer Science, Cornell University, 14853 Ithaca, NY. Email: damle@cornell.edu

like k -means clustering in an embedding space defined by the eigenvectors, instead of directly clustering in the original space.

In many of these cases, the relevant information is in the “leading” eigenvectors, *i.e.*, those corresponding to the k algebraically largest eigenvalues for some k (some methods, such as spectral clustering, use the k smallest, but simple shifting and scaling transformations make them the largest for a related matrix). For sufficiently large data sets computing a full eigendecomposition is prohibitively expensive, so we rely on iterative algorithms for computation. Perhaps the most well-known technique is the *power method* which dates back nearly a century; other common methods are subspace iteration and Krylov methods. Importantly, these methods only produce *approximations* to the eigenvectors. However, the approximation quality, as measured by subspace distance (effectively equivalent to using the ℓ_2 norm), is well-understood and there is well-established convergence analysis (Demmel, 1997; Golub and Van Loan, 2013; Parlett, 1998; Saad, 2011).

While spectral norm error analysis has been the standard-bearer for numerical analysis, recent statistical research has considered different subspace distance measures (Cai et al., 2019; Chen et al., 2018; Fan et al., 2018; Xia and Zhou, 2019). The motivation for these changes are statistical, as opposed to numerical: one observes a matrix $\tilde{A} = A + E$, where E is a source of noise and $A = \mathbb{E}[\tilde{A}]$ is the “population” version of A , containing the desired spectral information. We are then interested in $\|\tilde{u}_i \pm u_i\|_\infty$ as a distance measure between the eigenvectors of \tilde{A} and A . Here, the ℓ_∞ norm captures “entry-wise” error and is more appropriate when we care about maximum deviation; for example, when entries of the eigenvector are used to rank nodes or provide cluster assignments in a graph. This type of distance is often much smaller the spectral norm and, in contrast to the spectral norm, reveals information about the distribution of error over the entries. Recent theoretical results relate the noise E to the perturbation in the eigenvectors, as measured by ℓ_∞ norm or $\ell_{2 \rightarrow \infty}$ errors (Cape et al., 2019; Damle and Sun, 2019; Fan et al., 2018; Koltchinskii and Xia, 2016). Moreover, these results are often directly connected to machine learning problems such as clustering random graph models (Abbe et al., 2017; Eldridge et al., 2018).

The message from this body of literature is that when eigenvector entries are interpreted entry-wise, we should really measure our error entry-wise as well. This recent theoretical work shows what we can do *if* we have eigenvectors satisfying perturbation bounds in a different norm. Actually *computing* eigenvectors satisfying such error bounds is another question entirely. Current numerical algorithms typically use the ℓ_2 norm, and the motivation for norms like $\ell_{2 \rightarrow \infty}$ is that ℓ_2 can be a severe overestimate for the relevant approximation quality. Moreover, in contrast to the long history of research into stopping criteria for iterative methods in the unitarily-invariant setting (Arioli et al., 1992; Bai et al., 1993; Bennani and Braconnier, 1994; Golub and Meurant, 1997; Lehoucq et al., 1997), there are no generic stopping criteria closely tracking the quality of an approximation in the $\ell_{2 \rightarrow \infty}$ norm. For example, downstream tasks that depend on entrywise ordering, such as graph cluster quality obtained with an approximate Fiedler vector (Fairbanks et al., 2016) or spectral ranking via the Katz centrality (Nathan et al., 2017) employ ℓ_2 bounds, when instead the ℓ_∞ norm would constitute a better proxy. Some local spectral graph partitioning methods can be written as iteratively approximating an eigenvector in a (scaled) ℓ_∞ norm (Andersen et al., 2006), but these algorithms are far more specialized than general eigensolvers.

Here, we bridge this gap by providing an analysis for the convergence of subspace iteration, a widely-used iterative methods for computing leading eigenvectors, in terms of $\ell_{2 \rightarrow \infty}$ errors. As part of this, we provide a practical stopping criterion applicable to any iterative method for invariant subspace computation that tracks the $\ell_{2 \rightarrow \infty}$ error of the approximation. Our results show how, for a given error tolerance, one can perform many fewer subspace iterations to get the same desired performance on a downstream task that uses the eigenvectors (or, more generally, an invariant subspace). This reduction in iterations directly translates to substantial reductions in computation time. We demonstrate our methods with the help of applications involving real-world graph data, including node ranking in graphs, sweep cut profiles for spectral bipartitioning, and general spectral clustering.

1.1 Notation

We use the standard inner product on Euclidean spaces, defined by $\langle x, y \rangle := \text{Tr}(X^\top Y)$ for vectors/matrices X, Y . We write $\mathbb{O}_{n,k}$ for the set of matrices $U \in \mathbb{R}^{n \times k}$ such that $U^\top U = I_k$, dropping the second subscript when $n = k$. We use standard notation for norms, namely $\|A\|_2 := \sup_{x \in \mathbb{S}^{d-1}} \|Ax\|_2$ and $\|A\|_F := \sqrt{\langle A, A \rangle}$. Moreover, we remind the reader that the $\ell_\infty \rightarrow \ell_\infty$ operator norm for a matrix $A \in \mathbb{R}^{m \times n}$ is given by $\|A\|_\infty := \max_{i \in [m]} \|A_{i,:}\|_1$, where $A_{i,:}$ denotes the i^{th} row of A and $A_{:,i}$ denotes its i^{th} column. Finally, the $\ell_{2 \rightarrow \infty}$ norm is defined by

$$\|A\|_{2 \rightarrow \infty} := \sup_{x \in \mathbb{S}^{d-1}} \|Ax\|_\infty = \max_{i \in [m]} \|A_{i,:}\|_2. \quad (1)$$

Subspace distances. Given two orthogonal matrices $V, \tilde{V} \in \mathbb{O}_{n,r}$ inducing subspaces $\mathcal{V}, \tilde{\mathcal{V}}$, their so-called subspace distance is formally defined as

$$\text{dist}_2(V, \tilde{V}) := \|VV^\top - \tilde{V}\tilde{V}^\top\|_2 \quad (2)$$

and there are several equivalent definitions, *e.g.*, via the concept of *principal angles*, or via $\|V_\perp^\top \tilde{V}\|_2$, where V_\perp is a basis for the subspace orthogonal to \mathcal{V} . Here, in contrast, we will consider a slightly different notion of distance between subspaces with respect to $\|\cdot\|_{2 \rightarrow \infty}$ defined as

$$\text{dist}_{2 \rightarrow \infty}(V, \tilde{V}) := \inf_{O \in \mathbb{O}_{r,r}} \|V - \tilde{V}O\|_{2 \rightarrow \infty}. \quad (3)$$

This metric allows us to control errors in a “row-wise” or “entry-wise” sense; for example, in the case where $r = 1$ this reduces to infinity norm control over the differences between eigenvectors.

2 Convergence of subspace iteration

In this section, we analyze the convergence of subspace iteration with respect to the $\ell_{2 \rightarrow \infty}$ distance. In particular, we assume that we are working with a symmetric matrix A with eigenvalue decomposition

$$A = V\Lambda V^\top + V_\perp\Lambda_\perp V_\perp^\top, \quad (4)$$

where Λ, Λ_\perp are diagonal matrices containing the r largest and $n - r$ smallest eigenvalues of A . Throughout, we have the “blanket” assumption that we are interested in an incoherent subspace.

Algorithm 1 Subspace iteration

Input: $V^{(0)} \in \mathbb{O}_{n,k}$, symmetric matrix A , iterations T

$Q_0 := V^{(0)}$

for $t = 1, 2, \dots, T$ **do**

$V^{(t)} := AQ_{t-1}$

$Q_t, R_t = V^{(t)}$

▷ QR decomposition

end for

return Q_T

Assumption 1. *The subspace of interest $V \in \mathbb{O}_{n,r}$ is μ -incoherent:*

$$\max_{i \in [n]} \|VV^\top e_i\|_2 \leq \mu \sqrt{\frac{r}{n}}. \quad (5)$$

Subspace iteration with a fixed number of steps is given in Algorithm 1. For simplicity, we assume that the eigenvalues of the symmetric input A satisfy $\lambda_1(A) \geq \dots \geq \lambda_r(A) > \lambda_{r+1}(A) \geq \dots \geq \lambda_n(A)$ and, furthermore, that $\min_{k=1, \dots, r} |\lambda_k(A)| > \max_{k=r+1, \dots, n} |\lambda_k(A)|$.¹

The following result shows that $\text{dist}_{2 \rightarrow \infty}(Q_t, V)$ can be considerably smaller than $\text{dist}_2(Q_t, V)$. Unfortunately, the final result involves the unwieldy term $\|V_\perp \Lambda_\perp^t V_\perp^\top\|_\infty$, which is nontrivial to upper bound to obtain a better rate than that obtain using norm equivalence. To circumvent this, we impose an additional assumption.

Assumption 2. *For the matrix of interest, V_\perp satisfies*

$$\|V_\perp \Lambda_\perp^t V_\perp^\top\|_\infty \leq C \cdot \lambda_{r+1}^t \|V_\perp V_\perp^\top\|_\infty, \quad (6)$$

for a small constant C and all powers $t \in \mathbb{N}$.

Proposition 1. *Suppose Assumptions 1 and 2 hold. The iterates $\{Q_t\}$ produced by Algorithm 1 with initial guess Q_0 satisfy*

$$\begin{aligned} \text{dist}_{2 \rightarrow \infty}(Q_t, V) &\leq \left(\frac{\lambda_{r+1}}{\lambda_r}\right)^t \mu \sqrt{\frac{2r}{n}} \frac{d_0}{\sqrt{1-d_0^2}} \\ &\quad + \left(\frac{\lambda_{r+1}}{\lambda_r}\right)^t \frac{C(1+\mu\sqrt{r})}{\sqrt{1-d_0^2}} \text{dist}_{2 \rightarrow \infty}(Q_0, V), \end{aligned} \quad (7)$$

where $d_0 := \|Q_0^\top V_\perp\|_2 \equiv \text{dist}_2(Q_0, V)$ and $r = \dim(V)$.

Proof. Starting with the definition of the $2 \rightarrow \infty$ distance, we have

$$\begin{aligned} \text{dist}_{2 \rightarrow \infty}(Q_t, V) &= \inf_{Z \in \mathbb{O}_r} \|Q_t - VZ\|_{2 \rightarrow \infty} = \inf_{Z \in \mathbb{O}_r} \|(VV^\top + V_\perp V_\perp^\top)(Q_t - VZ)\|_{2 \rightarrow \infty} \\ &\stackrel{\text{\#}}{\leq} \sqrt{2} \|VV^\top\|_{2 \rightarrow \infty} \text{dist}_2(Q_t, V) + \|V_\perp V_\perp^\top\|_{2 \rightarrow \infty} \|Q_t - VZ\|_{2 \rightarrow \infty}, \end{aligned} \quad (8)$$

¹Our results hold for the largest magnitude eigenvalues assuming one defines the eigenvalue gap appropriately later, the simplification to the r algebraically largest eigenvalues being the largest in magnitude avoids burdensome notation without losing anything essential.

where (#) is due to the triangle inequality, followed by combining Lemmas A.2 and A.3. At this point, note that standard convergence results (Golub and Van Loan, 2013; Saad, 2011) state that

$$\text{dist}_2(Q_t, V) \leq \left(\frac{\lambda_{r+1}}{\lambda_r} \right)^t \frac{d_0}{\sqrt{1-d_0^2}},$$

and additionally Assumption 1 implies that $\|VV^\top\|_{2 \rightarrow \infty} \leq \mu\sqrt{r/n}$.

For the remainder, let us first recall a fact from the analysis of subspace iteration; the t^{th} iterate Q_t satisfies

$$\begin{aligned} Q_t R_t &= A^t V^{(0)}, \quad \text{with } R_t \text{ invertible} \\ \Rightarrow V_\perp^\top Q_t &= V_\perp^\top A^t V^{(0)} R_t^{-1} = \Lambda_\perp^t V_\perp^\top V^{(0)} R_t^{-1}. \end{aligned} \quad (9)$$

Then, notice that $V_\perp^\top V = 0$ and therefore we can rewrite the second term in (8) as

$$\begin{aligned} \|V_\perp V_\perp^\top Q_t\|_{2 \rightarrow \infty} &\stackrel{(*)}{=} \|V_\perp \Lambda_\perp^t V_\perp^\top Q_0 R_t^{-1}\|_{2 \rightarrow \infty} \stackrel{(b)}{=} \inf_{Z \in \mathbb{O}_r} \|V_\perp \Lambda_\perp^t V_\perp^\top (Q_0 - VZ) R_t^{-1}\|_{2 \rightarrow \infty} \\ &\stackrel{(c)}{\leq} \inf_{Z \in \mathbb{O}_r} C \|V_\perp V_\perp^\top\|_\infty \lambda_{r+1}^t \|(Q_0 - VZ) R_t^{-1}\|_{2 \rightarrow \infty} \\ &\leq C \|V_\perp V_\perp^\top\|_\infty \lambda_{r+1}^t \underbrace{\inf_{Z \in \mathbb{O}_r} \|Q_0 - VZ\|_{2 \rightarrow \infty}}_{=\text{dist}_{2 \rightarrow \infty}(Q_0, V)} \|R_t^{-1}\|_2, \end{aligned} \quad (10)$$

where (*) follows from Eq. (9), (b) holds since we can reintroduce VZ for any Z , as $V_\perp^\top V = 0$, (c) holds after combining Eq. (29) and Assumption 2, and the last inequality is Eq. (28). Notice that $\|R_t^{-1}\|_2 = \frac{1}{\sqrt{1-d_0^2}} \lambda_r^{-t}$, by tracing the proof of (Golub and Van Loan, 2013, Theorem 8.2.2).

Finally, by Lemma A.1, $\|V_\perp V_\perp^\top\|_\infty \leq 1 + \mu\sqrt{r}$. \square

When $\lambda_{r+2} \ll \lambda_{r+1}$, a slight modification of the above proof yields a potentially refined upper bound.

Proposition 2. *Under Assumption 1, the iterates $\{Q_t\}$ produced by Algorithm 1 with initial guess Q_0 satisfy*

$$\begin{aligned} \text{dist}_{2 \rightarrow \infty}(Q_t, V) &\leq \left(\frac{\lambda_{r+1}}{\lambda_r} \right)^t \mu \sqrt{\frac{2r}{n}} \cdot \frac{d_0}{\sqrt{1-d_0^2}} \\ &\quad + \left(\frac{\lambda_{r+2}}{\lambda_r} \right)^t \frac{d_0}{\sqrt{1-d_0^2}} + \frac{\|v_{r+1} v_{r+1}^\top\|_\infty}{\sqrt{1-d_0^2}} \left(\frac{\lambda_{r+1}}{\lambda_r} \right)^t \cdot \text{dist}_{2 \rightarrow \infty}(Q_0, V). \end{aligned} \quad (11)$$

Proof. For simplicity, let us define $\tilde{V} := [V \ v_{r+1}] \in \mathbb{R}^{n \times (r+1)}$ and \tilde{V}_\perp for the remaining $n - r - 1$ eigenvectors forming a basis of \mathbb{R}^n . Similarly, let $\tilde{\Lambda}_\perp = \text{diag}(\lambda_{r+2}, \dots, \lambda_n)$. From the definition of the $2 \rightarrow \infty$ distance, we have

$$\begin{aligned} \text{dist}_{2 \rightarrow \infty}(Q_t, V) &= \inf_{Z \in \mathbb{O}_r} \|Q_t - VZ\|_{2 \rightarrow \infty} = \inf_{Z \in \mathbb{O}_r} \|(VV^\top + V_\perp V_\perp^\top)(Q_t - VZ)\|_{2 \rightarrow \infty} \\ &\stackrel{(\#)}{\leq} \sqrt{2} \|VV^\top\|_{2 \rightarrow \infty} \text{dist}_2(Q_t, V) + \|V_\perp V_\perp^\top(Q_t - VZ)\|_{2 \rightarrow \infty} \end{aligned} \quad (12)$$

where (#) follows from Lemma A.2 in the main text and the fact that $\inf_{Z \in \mathbb{O}_r} \|Q_t - VZ\|_2 \leq \sqrt{2} \text{dist}_2(Q_t, V)$. Now we may rewrite the second term as

$$\begin{aligned} \|(v_{r+1}v_{r+1}^\top + \tilde{V}_\perp \tilde{V}_\perp^\top)Q_t\|_{2 \rightarrow \infty} &\leq \|v_{r+1}v_{r+1}^\top Q_t\|_{2 \rightarrow \infty} + \|\tilde{V}_\perp \tilde{V}_\perp^\top Q_t\|_{2 \rightarrow \infty} \\ &= \|v_{r+1}\lambda_{r+1}^t v_{r+1}^\top Q_0 R_t^{-1}\|_{2 \rightarrow \infty} + \|\tilde{V}_\perp \tilde{\Lambda}_\perp^t \tilde{V}_\perp^\top Q_0 R_t^{-1}\|_{2 \rightarrow \infty}. \end{aligned} \quad (13)$$

Pulling λ_{r+1}^t out of the first norm in (13) yields

$$\|v_{r+1}v_{r+1}^\top(Q_0 - VZ_\star)\|_{2 \rightarrow \infty} \|R_t^{-1}\|_2 \leq \|v_{r+1}v_{r+1}^\top\|_\infty \text{dist}_{2 \rightarrow \infty}(Q_0, V) \cdot \frac{\lambda_r^{-t}}{\sqrt{1-d_0^2}},$$

after using Lemma A.2 and the fact that $\|R_t^{-1}\|_2 \leq \frac{\lambda_r^{-t}}{\sqrt{1-d_0^2}}$, while the second norm in (13) can be upper bounded by

$$\|\tilde{V}_\perp \tilde{\Lambda}_\perp^t\|_2 \|\tilde{V}_\perp^\top Q_0\|_2 \|R_t^{-1}\|_2 = \left(\frac{\lambda_{r+2}}{\lambda_r}\right)^t \frac{\text{dist}_2(Q_0, \tilde{V})}{\sqrt{1-d_0^2}},$$

but as the respective subspaces satisfy $\mathcal{V} \subset \tilde{\mathcal{V}}$ we have $\text{dist}_2(Q_0, \tilde{V}) \leq \text{dist}_2(Q_0, V)$. Combining all the ingredients above completes the proof. \square

Propositions 1 and 2 show that we can achieve significant practical improvements, especially in the “typical” regime where $\text{dist}_{2 \rightarrow \infty}(Q_0, V) \ll \text{dist}_2(Q_0, V)$. Section 4 illustrates this concept in practical examples.

3 Stopping criteria

In this section, we propose and analyze a stopping criterion applicable when the desired convergence is with respect to the $2 \rightarrow \infty$ norm. Notably, this stopping criterion is generic and applicable to any iterative method for computing an invariant subspace.² Suppose that we have

$$AV - VS = E, \quad \|E\|_2 \leq \varepsilon, \quad V \in \mathbb{O}_{n,r}, \quad S = S^\top.$$

Then it is well-known (e.g., (Golub and Van Loan, 2013, Theorem 8.1.13)) that there exist $\mu_1, \dots, \mu_r \in \Lambda(A)$ such that

$$|\mu_k - \lambda_k(S)| \leq \sqrt{2}\varepsilon, \quad \forall k \in [r]. \quad (14)$$

This provides a handy criterion for testing convergence of eigenvalues, by setting $S = D_t$, the diagonal matrix of Ritz values at the t^{th} step and $V = Q_t$, the orthogonal matrix of Ritz vectors. One can, in fact, show the following:

²This includes Algorithm 1 and other common methods such as (block) Lanczos.

Lemma 1. Suppose that $A = A^\top \in \mathbb{R}^{n \times n}$ satisfies

$$AV - VS = E, \quad V^\top V = I_r, \quad (15)$$

for some **diagonal** matrix S . Then V is an invariant subspace of the matrix $A - EV^\top$.

Proof. By assumption, we have $VS = AV - E$ and therefore

$$(A - EV^\top)V = AV - EV^\top V = AV - E = VS,$$

which means that $(A - EV^\top)V_{:,i} = S_{i,i}V_{:,i}$, $\forall i \in [r]$, and $V_{:,i}$ are pairwise orthogonal. \square

We now demonstrate that checking $\|AV - VS\|_{\{2,2 \rightarrow \infty\}}$ leads to an appropriate stopping criterion for iterative methods for approximate eigenvectors, which simplifies under standard incoherence assumptions.³

Proposition 3. Assume that A is symmetric with V_1 as its dominant subspace and V_2 is the complement of V_1 , with $V_1 \in \mathbb{O}_{n,r}$; furthermore, suppose that A satisfies the conditions of Lemma 1 for some V and let gap be defined as in Theorem A.1. Then, if V is the leading invariant subspace of $A - EV^\top$ and $\|E\|_2 \leq \frac{\text{gap}}{5}$, we have

$$\begin{aligned} \text{dist}_{2 \rightarrow \infty}(V_1, V) &\leq 8 \|V_1\|_{2 \rightarrow \infty} \left(\frac{\|E\|_2}{\lambda_r - \lambda_{r+1}} \right)^2 \\ &\quad + 2 \|V_2 V_2^\top\|_\infty \frac{\|E\|_{2 \rightarrow \infty}}{\text{gap}} \cdot \left(1 + \frac{2 \|E\|_2}{\lambda_r - \lambda_{r+1}} \right). \end{aligned}$$

Proof. The condition on $\|E\|_2$ combined with the assumption that V is the leading invariant subspace of the perturbed matrix $A - EV^\top$ allows us to apply Theorem A.1 for the perturbation EV^\top , from which we deduce that the approximate eigenvector matrix V satisfies

$$\begin{aligned} \text{dist}_{2 \rightarrow \infty}(V_1, V) &\leq 8 \|V_1\|_{2 \rightarrow \infty} \left(\frac{\|E\|_2}{\lambda_r - \lambda_{r+1}} \right)^2 \\ &\quad + 2 \frac{\|V_2 V_2^\top EV^\top V_1\|_{2 \rightarrow \infty}}{\text{gap}} + 4 \frac{\|V_2 V_2^\top E\|_{2 \rightarrow \infty} \|E\|_2}{\text{gap} \cdot (\lambda_r - \lambda_{r+1})} \end{aligned}$$

with the appropriate definition of gap . Using Lemma A.2, we can upper bound the terms above as

$$\|V_2 V_2^\top EV^\top V_1\|_{2 \rightarrow \infty} \leq \|V_2 V_2^\top\|_\infty \|EV^\top V_1\|_{2 \rightarrow \infty} \leq \|V_2 V_2^\top\|_\infty \|E\|_{2 \rightarrow \infty} \underbrace{\|V^\top V_1\|_2}_{\leq 1},$$

and similarly for the term $\|V_2 V_2^\top E\|_{2 \rightarrow \infty}$. \square

Corollary 1. Suppose that $V_1 \in \mathbb{O}_{n,r}$ is μ -incoherent and the conditions of Proposition 1 are satisfied with $\|E\|_2 \leq \varepsilon_1$, $\|E\|_{2 \rightarrow \infty} \leq \varepsilon_2$. Then the approximate eigenvector matrix V satisfies

$$\text{dist}_{2 \rightarrow \infty}(V, V_1) \leq 8\mu \sqrt{\frac{r}{n}} \left(\frac{\varepsilon_1}{\lambda_r - \lambda_{r+1}} \right)^2 + 2 \frac{1 + \mu\sqrt{r}}{\text{gap}} \cdot \left(\varepsilon_2 + 2 \frac{\varepsilon_1 \varepsilon_2}{\lambda_r - \lambda_{r+1}} \right),$$

with gap defined as in Theorem A.1.

³As the perturbed matrix is non-normal, an eigengap condition does not suffice to guarantee that V is the leading invariant subspace of the perturbed matrix. To invoke Proposition 3 with the approximate eigenvectors in the place of V , one relies on the fact that V approaches V_1 by convergence theory of subspace iteration.

Practical issues. Checking the criterion of Corollary 1 when running Algorithm 1 has two ingredients: computing $\|E\|_{\{2,2 \rightarrow \infty\}}$, and estimating gap. Computing the $2 \rightarrow \infty$ norm is straightforward, while $\|E\|_2$ can be well-approximated by a few Krylov iterations. To estimate gap, in practice we assume that $\text{sep}_{2 \rightarrow \infty, V_2}(\Lambda_1, V_2 \Lambda_2 V_2^\top)$ is (at worst) a small multiple of the $\lambda_r - \lambda_{r+1}$. To estimate $\lambda_r - \lambda_{r+1}$, we may use a combination of techniques, such as augmenting the “seed” subspace by a constant number of columns and setting $|\lambda_r - \lambda_{r+1}| \approx \hat{\lambda}_r - \hat{\lambda}_{r+1}$, since it is well known that eigenvalue estimates converge at a quadratic rate for symmetric matrices (Stewart, 1969).

In the absence of incoherence information, we can replace all quantities in the residual by estimates. For any compatible B , $\|BV_1\|_{2 \rightarrow \infty} = \|BV_1 V_1^\top\|_{2 \rightarrow \infty}$ by (30), which we may replace with $\|BV\|_{2 \rightarrow \infty}$, as $V_1 V_1^\top \approx V V^\top$ after sufficient progress. Similarly, we can write $V_2 V_2^\top = I - V_1 V_1^\top \approx I - V V^\top$, to obtain the approximated residual (at iteration t , with $V \equiv Q_t$):

$$\begin{aligned} \text{res}_{2 \rightarrow \infty}(t) &\approx 8 \|Q_t\|_{2 \rightarrow \infty} \left(\frac{\|E\|_2}{\lambda_r - \lambda_{r+1}} \right)^2 \\ &\quad + 2 \frac{\|(I - Q_t Q_t^\top)E\|_{2 \rightarrow \infty}}{\text{gap}} \cdot \left(1 + 2 \frac{\|E\|_2}{\lambda_r - \lambda_{r+1}} \right) \end{aligned} \quad (16)$$

The main drawback of using Equation (16) is that the substitutions used above are not accurate until $Q_t Q_t^\top$ is sufficiently close to $V_1 V_1^\top$. This is observed empirically in Section 4, as $\text{res}_{2 \rightarrow \infty}(t)$ is looser than average in the first few iterations.

Another practical concern is evaluating the quality of the bound in Corollary 1; formally, there is no known method for computing $Z_\star := \text{argmin}_{Z \in \mathbb{O}_r} \|\hat{V} - VZ\|_{2 \rightarrow \infty}$ in closed form or via some globally convergent iterative method. We use a proxy for tracking the behavior of the $\ell_{2 \rightarrow \infty}$ distance. In particular, we use

$$Z_F = \text{argmin}_{Z \in \mathbb{O}_r} \|\hat{V} - VZ\|_F, \quad (17)$$

an instance of the so-called *orthogonal Procrustes problem*, whose solution can be obtained via the SVD of $V^\top \hat{V}$ (Higham, 1988). It is then straightforward to show the following:

Corollary 2. *Let Z_F be the solution of the orthogonal Procrustes problem from (17). The iterates $\{Q_t\}$ produced by Algorithm 1 with initial guess Q_0 satisfy (under Assumptions 1 and 2):*

$$\begin{aligned} \|Q_t - VZ_F\|_{2 \rightarrow \infty} &\leq 2\mu \frac{r}{\sqrt{n}} \left(\frac{\lambda_{r+1}}{\lambda_r} \right)^t \frac{d_0}{\sqrt{1 - d_0^2}} \\ &\quad + \left(\frac{\lambda_{r+1}}{\lambda_r} \right)^t \frac{C(1 + \mu\sqrt{r})}{\sqrt{1 - d_0^2}} \text{dist}_{2 \rightarrow \infty}(Q_0, V) \end{aligned} \quad (18)$$

Proof. Tracing the proofs of Proposition 1, we bound the $\ell_{2 \rightarrow \infty}$ distance above by

$$\inf_{Z \in \mathbb{O}_r} \|Q_t - VZ\|_{2 \rightarrow \infty} \leq \|Q_t - VZ_F\|_{2 \rightarrow \infty} \leq \mu \sqrt{\frac{r}{n}} \|Q_t - VZ_F\|_2 + \|V_\perp V_\perp^\top Q_t\|_{2 \rightarrow \infty},$$

where the second term can be analyzed as before. For the first term, let us denote $Z_2 := \operatorname{argmin}_{Z \in \mathbb{O}_r} \|Q_t - VZ\|_2$ and observe that we can upper bound

$$\|Q_t - VZ_F\|_2 \stackrel{(1)}{\leq} \|Q_t - VZ_F\|_F \stackrel{(2)}{\leq} \|Q_t - VZ_2\|_F \stackrel{(3)}{\leq} \sqrt{2r} \|Q_t - VZ_2\|_2 \quad (19)$$

$$\stackrel{(4)}{\leq} 2\sqrt{r} \cdot \operatorname{dist}_2(Q_t, V) = 2\sqrt{r} \left(\frac{\lambda_{r+1}}{\lambda_r} \right)^t \frac{d_0}{\sqrt{1 - d_0^2}}, \quad (20)$$

where (1) is since $\|X\|_2 \leq \|X\|_F$, $\forall X$, (2) is by the definition of Z_F , (3) uses the fact that $\operatorname{rank}(Q_t - VZ) \leq 2r$ by definition and norm equivalence, and step (4) follows from Lemma A.3. \square

Therefore, the oft-used proxy $\|\hat{V} - VZ_F\|_{2 \rightarrow \infty}$ enjoys a similar convergence guarantee with an additional multiplicative factor that is typically small compared to n (a similar rate can be shown for Proposition 2 using the same argument as above). This is precisely the $2 \rightarrow \infty$ distance we report in the forthcoming experiments and is in alignment with the approach of Damle and Sun (2019), who study the effect of perturbations on the $\ell_{2 \rightarrow \infty}$ subspace distance via the solution to (17).

4 Applications

In this section, we present a set of numerical experiments illustrating the results of our analysis in practice, as well as the advantages of the proposed stopping criterion. Importantly, in our applications, *entry-wise* error is the natural criterion, often because what matters for the downstream task is an ordering induced by computed eigenvectors.

4.1 Synthetic examples

To verify our theory and get a sense of the tightness of our bounds on convergence rates, we first test on synthetic data. To this end, we implemented Algorithm 1 in Julia (Bezanson et al., 2017) and generated matrices as follows, given a matrix dimension n and subspace dimension r :

1. Sample a random matrix from $\mathbb{O}_{n,n}$ uniformly at random (see (Mezzadri, 2007) for details); select r of its columns uniformly at random to form Q .
2. generate $\lambda_i \equiv \rho^{i-1}$, for a decay factor $\rho = 0.95$.
3. Form $A = [Q \ Q_\perp] \Lambda [Q \ Q_\perp]^\top$, where Q_\perp is any matrix in $\mathbb{O}_{n,n-r}$ orthogonal to Q . We initialize Q_\perp to be a random subset of the columns of the identity matrix, and orthogonalize it against Q .

We compare distances and residuals for synthetic examples with $n = 5000$ and $r = 50$ and various stopping thresholds ε for the residuals (Figure 1). While the ℓ_2 norm residual closely tracks the corresponding distance, the residual from Equation (16) overshoots by a small multiplicative factor, suggesting that the large constants in Proposition 3 may only be necessary in pathological cases and could be reduced in practice. Moreover, the $\ell_{2 \rightarrow \infty}$ norm residual can substantially overestimate the actual distance in the first few iterations, as the estimate of

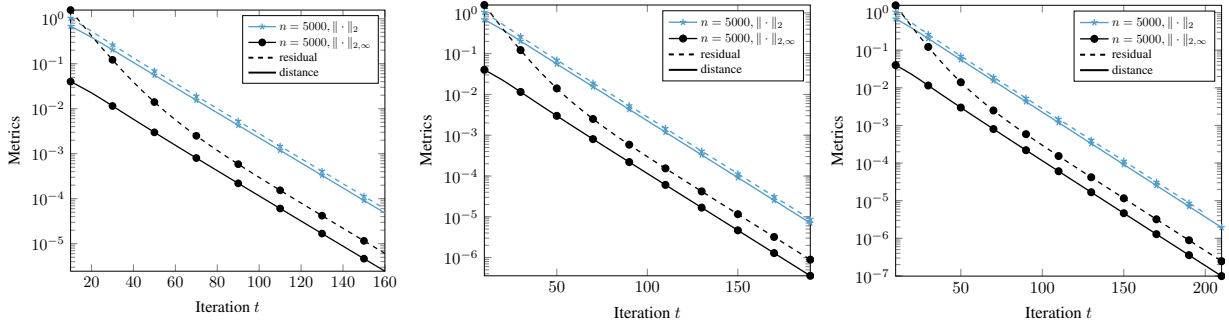


Figure 1: Distances (**solid** lines) and residuals (**dashed** lines) for synthetic examples with $r = 50$ and target accuracies $\varepsilon = 10^{-4}$ (**left**), $\varepsilon = 10^{-5}$ (**middle**) and $\varepsilon = 10^{-6}$ (**right**).

Equation (16) depends on $Q_t Q_t^\top$ not being “too far” from VV^\top . The gap narrows after a few dozen iterations.

In addition, we examine the looseness of the bounds from Propositions 1 and 2 for the same experiment (Figure 2). We evaluate the following rates:

$$\begin{aligned}
 \text{rate}_1(t) &:= \left(\frac{\lambda_{r+1}}{\lambda_r} \right)^t \cdot \frac{\text{dist}_{2 \rightarrow \infty}(Q_0, V)}{\sqrt{1 - d_0^2}}, \\
 \text{rate}_2(t) &:= \text{rate from Proposition 2}, \\
 \text{rate}_3(t) &:= \text{rate from Proposition 1}, \\
 \text{rate}_{\text{naive}}(t) &:= \left(\frac{\lambda_{r+1}}{\lambda_r} \right)^t \frac{d_0}{\sqrt{1 - d_0^2}}
 \end{aligned} \tag{21}$$

Here, rate_1 is an idealized rate that we would like to hold as an analog of the classical convergence results for the ℓ_2 norm (Golub and Van Loan, 2013, Theorem 8.2.2). Via Proposition 1, rate_3 uses incoherence and a decay relationship involving spectral projectors and λ_{r+1} , whereas rate_2 only uses incoherence but depends on λ_{r+2}/λ_r . The naive rate uses an ℓ_2 subspace distance. In all the synthetic examples we generated, Assumption 2 was verified to hold with constant $C < 1.5$.

Remarkably, for a range of dimensions n and r we find that rate_3 (which uses Proposition 1) closely tracks the “idealized” rate_1 on these synthetic matrices (Fig. 2). Also, rate_2 (which uses Proposition 2) is a looser upper bound. This agrees with our theoretical analysis, as λ_{r+2} is only moderately smaller than λ_{r+1} in our synthetic matrix construction. Finally, as expected, the naive rate is the loosest bound.

4.2 Eigenvector centrality

Next, we develop an experiment for network centrality, where the task is to measure the influence of nodes in a graph (Newman, 2008). Each node is assigned a score, which is a function of the graph topology, and a typical underlying (recursive) assumption is that a node with a high score contributes a larger influence to other nodes to which it is connected. Here, we consider *eigenvector centrality*, which is one the standard measures in network science. Given a graph

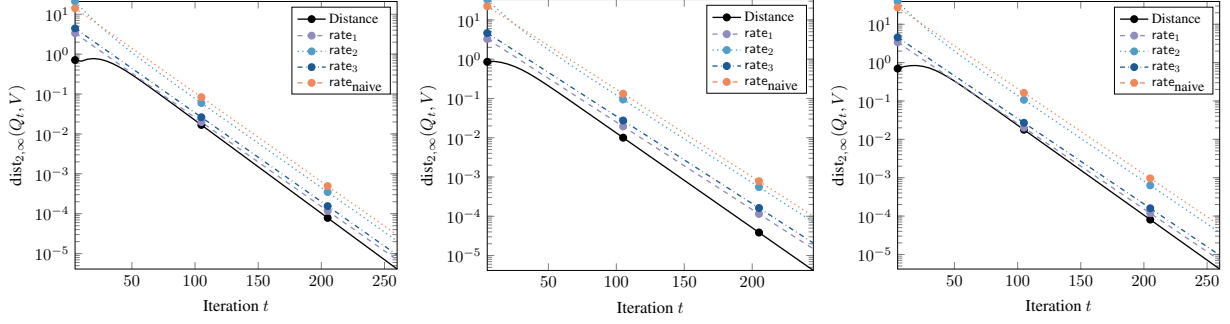


Figure 2: Distance (solid lines) and convergence rates from Equation (21) for matrix and subspace dimensions $(n, r) = (1000, 10)$ (left); $(3500, 15)$ (middle); and $(8000, 20)$ (right). Here, rate_1 is an idealized rate based on an analog of the classical convergence, which is the best one could hope to achieve. Our rate_3 from Proposition 1 tracks this idealized closely in the synthetic data examples.

$G = (V, E)$; the eigenvector centrality score of a node u , $x_u > 0$, is defined as a solution to the following equation:

$$x_u := \frac{1}{\lambda} \sum_{v \in V} A_{uv} x_v, \quad A_{uv} := \begin{cases} 1, & \text{if } u \text{ links to } v \\ 0, & \text{otherwise} \end{cases}, \quad (22)$$

where λ is a proportionality constant. Here, node u 's scores depend linearly on all of its neighbors' scores. Under the positivity requirement of x_u and provided that the graph is connected, rearranging and the Perron-Frobenius theorem show that $x = v_1$, the eigenvector corresponding to the largest eigenvalue λ_1 of A (up to scaling). In this setting, we are typically interested in the *ordering* of nodes produced by the centrality score and not the actual scores themselves (e.g., to determine the influential or non-influential nodes). Therefore, the $\ell_{2 \rightarrow \infty}$ distance, which measures $\|v_1 - \hat{v}_1\|_\infty$, is more appropriate than $\|v_1 - \hat{v}_1\|_2$ as a proxy for the quality of the estimate \hat{v}_1 . To get a correct ranking result, it suffices to have $\|v_1 - \hat{v}_1\|_\infty < (1/2) \cdot \min_{i,j} |v_i - v_j|$. On the other hand, $\|\hat{v}_1 - v_1\|_2$ does not have an interpretable criterion.

We demonstrate the above principle by comparing two stopping criteria: the criterion from Equation (16) with a specified threshold ε against the “naive” way of stopping when $\|A\hat{v}_1 - \hat{\lambda}\hat{v}_1\|_2 \leq \hat{\lambda}\varepsilon$, where $\hat{\lambda}$ is the current eigenvalue estimate. If a user specifies a tolerance ε , we expect that using our $\ell_{2 \rightarrow \infty}$ error measurements and our corresponding stopping criteria will tell us that we can be confident in our solution much more quickly.

This is indeed the case — using our methodology provides a substantial reduction in computation time on a variety of real-world graphs, whose summary statistics are in Table 1. Figure 3 shows the ratio between the two quantities t_{comp} and t_{naive} , defined as

$$\begin{aligned} t_{\text{comp}} &:= \min \{t > 0 \mid \text{res}_{2 \rightarrow \infty}(t) \leq \varepsilon\} \\ t_{\text{naive}} &:= \min \{t > 0 \mid \|A\hat{V}_{:,j} - \hat{\lambda}_j \hat{V}_{:,j}\| \leq \varepsilon \hat{\lambda}_j, \forall j\} \end{aligned} \quad (23)$$

These are the stopping times for satisfying the residual criterion from Equation (16) and the “naive” ℓ_2 residual criterion at a given level, respectively. In the low-to-medium accuracy regimes,

Table 1: Summary statistics of network datasets.

Dataset	# nodes	# edges
CA-HEPPH	11204	117649
CA-ASTROPH (Leskovec et al., 2005)	17903	197031
GEMSEC-FACEBOOK-ARTIST (Rozemberczki et al., 2019)	50515	819306
COM-DBLP	317080	1049866
COM-LIVEJOURNAL (Yang and Leskovec, 2012)	3997962	34681189

using our stopping method results in least 20 – 40% reductions in the number of iterations needed. In this regime, the ranking induced by the approximate eigenvector had typically already converged to the “true” ordering obtained by computing the eigenvector to machine precision. To measure ranking, we defined

$$\text{dist}_\tau(v_1, v_2) := \frac{1 - \tau(v_1, v_2)}{2} \in [0, 1], \quad (24)$$

where $\tau(v_1, v_2)$ is *Kendall’s τ -correlation* (Kendall, 1948) between the ranking induced by sorting the entries of v_1 and v_2 ; it’s straightforward to check that when v_1, v_2 induce the same ranking, $\text{dist}_\tau(v_1, v_2) = 0$, while $\text{dist}_\tau(v_1, v_2) = 1$ when the rankings are most dissimilar. Figure 4 (right) shows the behavior of the different distance measures when applying our pipeline to various graphs from the SNAP network collection, where it is apparent that a moderate threshold of roughly 10^{-4} yields the correct ranking in all cases.

4.3 Spectral clustering in graphs

Another downstream task employing invariant subspaces is spectral clustering, which we study here as a way to partition a graph into well-separated “communities” or “clusters”. The standard pipeline is to compute the leading r -dimensional eigenspace of the normalized adjacency matrix $A_N = D^{-1/2}AD^{-1/2}$, where r is the desired number of clusters, D is the diagonal degree matrix, and A is the adjacency matrix. The resulting eigenvector matrix provides an r -dimensional embedding for each node, which is subsequently fed to a point cloud clustering algorithm such as `k-means` (Von Luxburg, 2007). For our experiment, we employ the deterministic QR-based algorithm from (Damle et al., 2018) on the same set of real-world graphs that we used for eigenvector centrality. Since the algorithm of (Damle et al., 2018) is deterministic, we do not have to worry about randomness pertaining to initialization (e.g. as in `k-means++`), and only run the experiment once for each configuration of parameters.

In this setup, the eigenvectors (more carefully, a rotation of them) are approximate cluster indicators. Indeed, spectral clustering on graphs is often derived from a continuous relaxation of

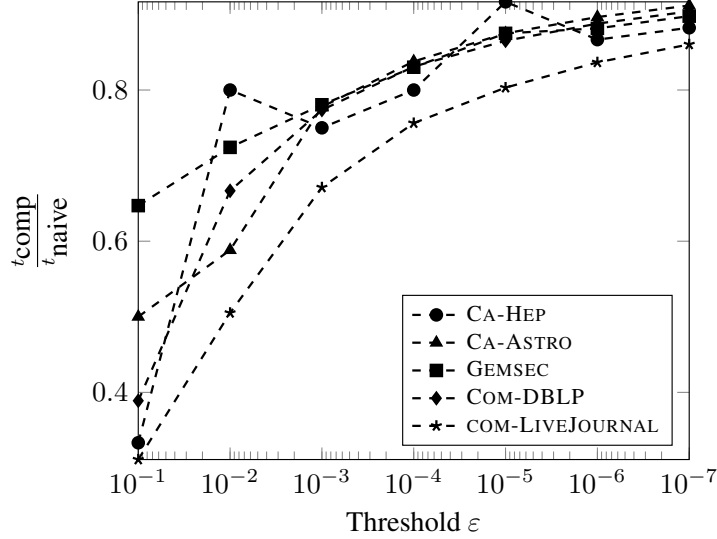


Figure 3: Ratio of the number of iterations needed to satisfy $\text{res}_{2 \rightarrow \infty}(t) \leq \varepsilon [t_{\text{comp}}]$ over the number of iterations for the “naive” criterion $\|A\hat{v} - \hat{\lambda}\hat{v}\|_2 \leq \varepsilon \hat{\lambda} [t_{\text{naive}}]$, for thresholds $\varepsilon = 10^{-k}$, in computing the eigenvector centrality to rank the top $\lfloor \sqrt{n} \rfloor$ nodes in a graph. Our analysis and stopping criteria enable significantly fewer iterations.

a combinatorial objective based on these indicators (Von Luxburg, 2007). Thus, we are once again interpreting the eigenvectors entry-wise, and $\ell_{2 \rightarrow \infty}$ error is a more sensible metric than ℓ_2 error. This fact has been used to analyze random graph models with cluster structure (Lyzinski et al., 2014).

For all the datasets involved, we hand-pick the target number of clusters r by inspecting the successive ratios of the leading few eigenvalues and setting r so that the ratio $\frac{\lambda_{r+1}}{\lambda_r}$ is small, but also taking into account the fact that we don’t want r to be too small. Additionally, we use the regularized version of the normalized adjacency matrix A_ρ (Amini et al., 2013), which augments the adjacency and degree matrices A, D using a regularization parameter ρ :

$$A_\rho := A + \frac{\rho}{n} \mathbf{1}\mathbf{1}^\top, \quad D_\rho := D + \rho \quad (25)$$

Following standard practice (Qin and Rohe, 2013; Zhang and Rohe, 2018), we set ρ equal to a constant which is near the average degree of the graph and then perform the eigendecomposition of

$$\tilde{A}_\rho = D_\rho^{-1/2} A_\rho D_\rho^{-1/2} + I,$$

shifting by $+I$ to ensure that the algebraically largest eigenvalues are also the largest in magnitude, in order for subspace iteration to be applicable. We summarize the hyperparameter choices for each dataset in Table 2.

In the same manner as the eigenvector centrality experiment, we compare the ratio of iteration counts: t_{comp} over t_{naive} , as defined in Equation (23) (Figure 5, left). In this case, we see even larger savings. For ε around 10^{-2} , our stopping criterion results in 70–80% savings in computation time. While this approximation level may seem crude at first, we can measure

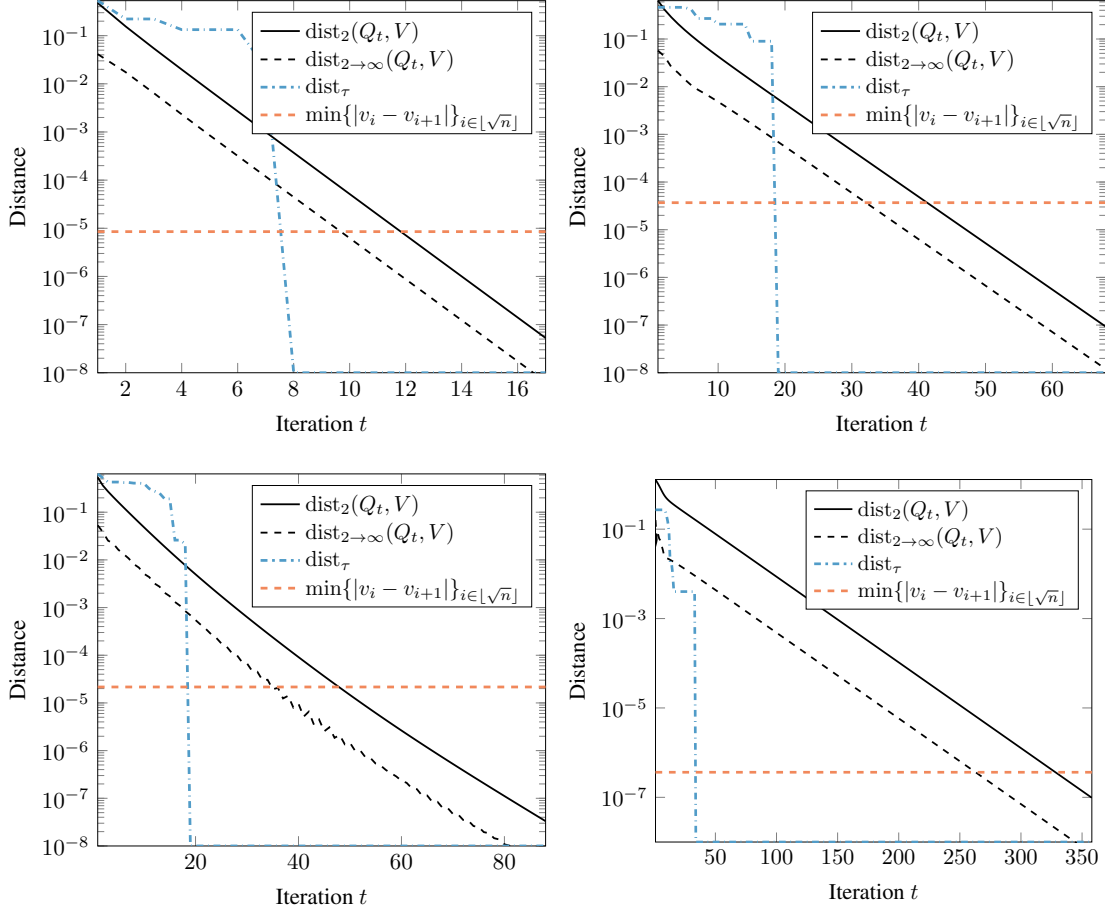


Figure 4: Distance metrics for approximating the eigenvector centrality of several graphs to rank their top $\lfloor \sqrt{n} \rfloor$ nodes. **Datasets** (clockwise): CA-HEPPH, CA-ASTROPH, COM-LIVEJOURNAL, GEMSEC.

the performance of the algorithms in terms of the *normalized cut* metric, for which spectral clustering is a continuous relaxation (Von Luxburg, 2007). Given a partition of the vertex set V into S_1, \dots, S_k , which correspond to the different communities, we define⁴

$$\text{ncut}(S_1, \dots, S_k) := \frac{1}{2} \sum_{i=1}^k \phi(S_i), \quad \phi(S_i) := \frac{\sum_{i \in S, j \notin S} A_{ij}}{\sum_{i \in S} \sum_{j \in V} A_{ij}} \quad (26)$$

We find that by the time we reach residual level $\varepsilon = 10^{-2}$, the cut value found using the approximate subspace is essentially the same as the one using the subspace computed to numerical precision (see right of Figure 5).

⁴Note that the definition of ϕ used here is slightly different than the one used in the experiments of Section 4.4.

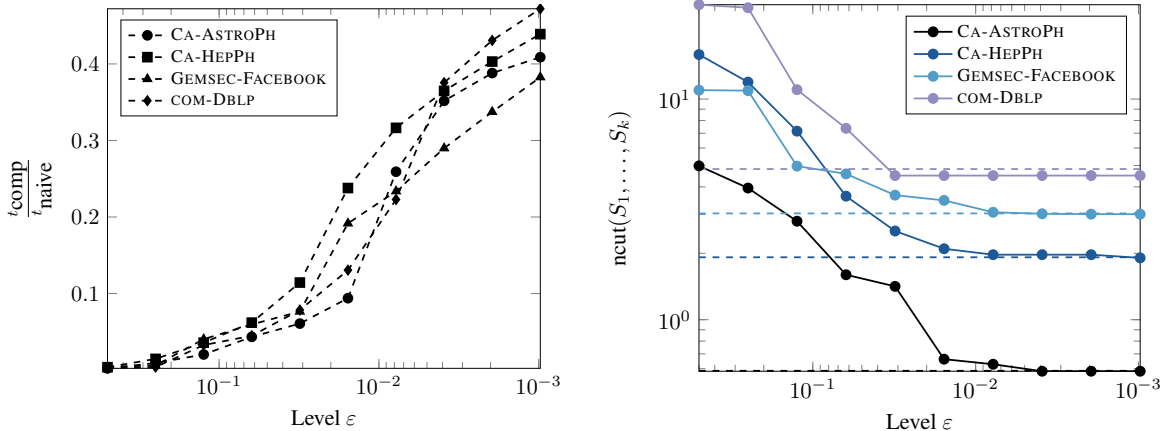


Figure 5: Spectral clustering on various datasets. **Left:** Ratio of iteration counts needed to satisfy $\text{res}_{2 \rightarrow \infty}(t) \leq \epsilon [t_{\text{comp}}]$ over number of iterations for the “naive” criterion $\|A\hat{v} - \hat{\lambda}\hat{v}\|_2 \leq \epsilon \hat{\lambda} [t_{\text{naive}}]$. **Right:** Normalized cut metric at different levels ϵ . Our analysis and stopping criteria enable significantly fewer iterations without sacrificing performance in the underlying task.

Table 2: Parameters for spectral clustering

Dataset	# of clusters r	ρ
CA-HEPPH	17	1.0
CA-ASTROPH	6	1.0
GEMSEC	12	1.0
DBLP	28	5.0

4.4 Spectral bipartitioning and sweep cuts

Another spectral method for finding clusters in graphs is spectral bipartitioning, which aims to find a single cluster of nodes S with small conductance $\phi(S)$:

$$\phi(S) := \frac{\sum_{i \in S, j \notin S} A_{ij}}{\min(A(S), A(S^c))}, \quad A(S) := \sum_{i \in S} \sum_{j \in V} A_{ij}.$$

The conductance objective is a standard measure for identifying a good cluster of nodes (Leskovec et al., 2008; Schaeffer, 2007): if $\phi(S)$ is small, there are not many edges leaving S and there are many edges contained in S .

Minimizing $\phi(S)$ is NP-hard, but a spectral method provides guarantees. The method computes the eigenvector v_2 corresponding to the second largest eigenvalue of the normalized adjacency matrix, which is often called the *Fiedler vector* (Fiedler, 1973). To find the a set with small conductance, the method uses the so-called “sweep cut”. After scaling v_2 by the inverse square root of degrees, we sort the nodes by their value in the eigenvector, and then consider the top- k nodes as a candidate set S for all values of k . The value of k that gives the smallest conductance produces a set S satisfying $\phi(S) \leq 2\sqrt{\min_{S'} \phi(S')}$, which is the celebrated Cheeger inequality (Chung, 1997).

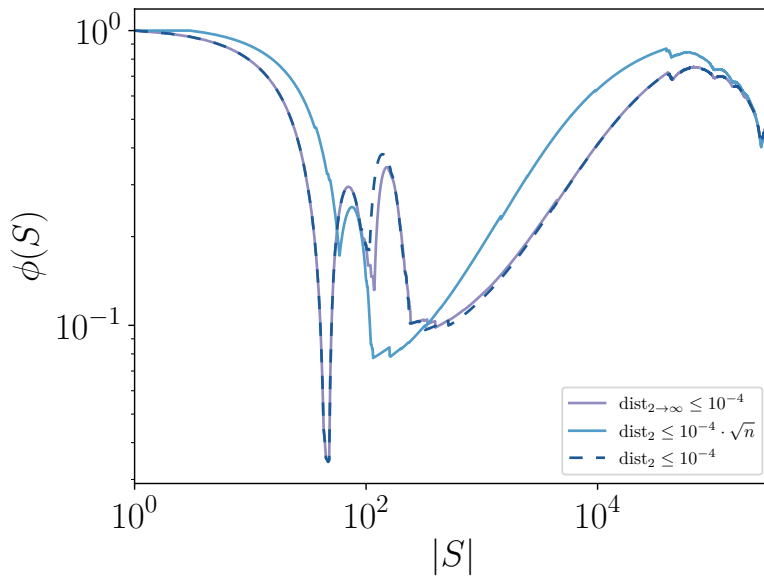


Figure 6: Sweep cut profile (cut conductance vs. cardinality) for COM-DBLP. For a fixed ε , our $\ell_{2 \rightarrow \infty}$ stopping criterion leads to faster convergence. Increasing the tolerance for ℓ_2 by the norm equivalence factor produces lower-quality solutions. Here $t_{\text{comp}} = 1135$ vs. $t_{\text{naive}} = 1378$ iterations.

As in the case of eigenvector centrality, what matters is the *ordering* induced by the eigenvector. Thus, a $\ell_{2 \rightarrow \infty}$ stopping criterion is again more appropriate than a standard ℓ_2 one. As a heuristic, one might consider just making ℓ_2 tolerance larger. We have seen that the spectral norm distance can be a factor of \sqrt{n} loose compared to the $\ell_{2 \rightarrow \infty}$ distance. Thus, we could use ε for $\ell_{2 \rightarrow \infty}$ and $\sqrt{n}\varepsilon$ for ℓ_2 . However, this can substantially reduce the solution quality; moreover, we expect such effects to become even more pronounced as the problem dimension n increases.

We illustrate this in Fig. 6, where we plot the conductance values obtained in the sweep cut as a function of the size of the set on COM-DBLP. This is a sweep cut approximation of a network community profile plot (Benson et al., 2016; Leskovec et al., 2008), which visualizes cluster structure at different scales. Using the naive ℓ_2 stopping criterion provides the same solution quality but requires more iterations. In the case of $\varepsilon = 10^{-4}$ in Fig. 6, our methods produce 20% computational savings. Finally, the heuristic $\sqrt{n}\varepsilon$ tolerance for the ℓ_2 stopping criterion produces a cruder solution and finds a set with larger conductance.

5 Conclusions

The broad applicability of spectral methods, coupled with the prevalence of entry-wise interpretations of eigenvectors (or row-wise interpretations to invariant subspaces) strongly motivates imbuing our computational methods with appropriate stopping criteria. Our theoretical results demonstrate just how much smaller the $\ell_{2 \rightarrow \infty}$ subspace distance can be than traditional measures, an observation supported by experiment. In fact, the accuracy with which we compute eigenvectors can have a non-trivial impact on downstream applications — if we would like use fewer

iterations to save time we must do so carefully, and our new stopping criterion provides an easy to implement way to do this that comes at essentially no cost and with strong guarantees.

Acknowledgments

This research was supported by NSF Award DMS-1830274, ARO Award W911NF19-1-0057, and ARO MURI.

A Auxiliary Results

Lemma A.1 (Incoherence). *Consider a subspace \mathcal{V} of dimension r and its spectral projector VV^\top . If V is μ -incoherent, i.e., $\|VV^\top\|_{2 \rightarrow \infty} \leq \mu\sqrt{\frac{r}{n}}$, then for its complementary subspace \mathcal{V}_\perp it holds that*

$$\|V_\perp V_\perp^\top\|_\infty \leq (1 + \mu\sqrt{r}).$$

Proof. Observe that $\|A\|_\infty \leq \sqrt{n} \|A\|_{2 \rightarrow \infty}$. Thus,

$$\begin{aligned} \|V_\perp V_\perp^\top\|_\infty &= \|I - VV^\top\|_\infty \leq 1 + \|VV^\top\|_\infty \\ &\leq 1 + \sqrt{n} \|VV^\top\|_{2 \rightarrow \infty} \leq 1 + \sqrt{n}\mu\sqrt{r/n}. \end{aligned}$$

□

The next theorem, originally stated without assuming symmetry, is adapted for the case of a symmetric initial matrix.

Theorem A.1 (Theorem 5.1 in (Damle and Sun, 2019)). *Suppose $\tilde{A} = A + E$ with A symmetric, having eigenvalue decomposition $A = V_1\Lambda_1V_1^\top + V_2\Lambda_2V_2^\top$, where $V_1 \in \mathbb{R}^{n \times r}$, $V_2 \in \mathbb{R}^{n \times (n-r)}$ have orthonormal columns. Moreover, let*

$$\text{gap} := \min \{ \lambda_r - \lambda_{r+1}, \text{sep}_{2 \rightarrow \infty, V_2}(\Lambda_1, V_2\Lambda_2V_2^\top) \},$$

with $\text{sep}_{2 \rightarrow \infty, V_2}$ defined as the following quantity:

$$\text{sep}_{2 \rightarrow \infty, V_2}(A, B) := \inf \{ \|AZ - ZB\|_{2 \rightarrow \infty} \mid Z \in \text{ran}(V_2), \|Z\|_{2 \rightarrow \infty} = 1 \}$$

If $\|E\|_2 \leq \frac{\text{gap}}{5}$, then the leading invariant subspace of \tilde{A} , \tilde{V}_1 , satisfies

$$\begin{aligned} \inf_{O \in \mathbb{O}_r} \|\tilde{V}_1 - V_1O\|_{2 \rightarrow \infty} &\leq 8 \|V_1\|_{2 \rightarrow \infty} \left(\frac{\|E\|_2}{\lambda_r - \lambda_{r+1}} \right)^2 \\ &+ 2 \frac{\|V_2V_2^\top EV_1\|_{2 \rightarrow \infty}}{\text{gap}} + 4 \frac{\|V_2V_2^\top E\|_{2 \rightarrow \infty} \|E\|_2}{\text{gap} \cdot (\lambda_r - \lambda_{r+1})}. \end{aligned} \tag{27}$$

Lemma A.2 (Cape et al. (2019)). *We have*

$$\|AB\|_{2 \rightarrow \infty} \leq \|A\|_{2 \rightarrow \infty} \|B\|_2 \tag{28}$$

$$\|AB\|_{2 \rightarrow \infty} \leq \|A\|_\infty \|B\|_{2 \rightarrow \infty} \tag{29}$$

Moreover, for any matrix V with orthonormal columns, it holds that

$$\|AV^\top\|_{2 \rightarrow \infty} = \|A\|_{2 \rightarrow \infty}. \tag{30}$$

While we believe the result of Lemma A.3 may be folklore, we were unable to locate a reference for it, and provide a proof for completeness.

Lemma A.3. *We have $\inf_{Z \in \mathbb{O}_r} \|\tilde{V} - VZ\|_2 \leq \sqrt{2} \text{dist}_2(V, \tilde{V})$.*

Proof. Recall the solution of the orthogonal Procrustes problem, given by the SVD of $V^\top \tilde{V}$, $U\Sigma W^\top$. Since $UW^\top \in \mathbb{O}_r$, with $U^\top U = UU^\top = W^\top W = WW^\top = I_r$, we have

$$\begin{aligned} \inf_{Z \in \mathbb{O}_r} \|\tilde{V} - VZ\|_2 &\leq \|\tilde{V} - VUW^\top\|_2 = \sqrt{\sup_x \langle x, (\tilde{V} - VUW^\top)^\top (\tilde{V} - VUW^\top) x \rangle} \\ &= \sqrt{\sup_x \langle x, (I - \tilde{V}^\top VUW^\top - WU^\top V^\top \tilde{V} + I) x \rangle} \\ &\stackrel{(\sharp)}{=} \sqrt{\sup_x \langle x, 2(I - W\Sigma W^\top) x \rangle} = \sqrt{2} \|I - W\Sigma W^\top\|_2 \\ &= \sqrt{2} \sqrt{\|I - \Sigma\|_2} = \sqrt{2} \sqrt{1 - \sigma_r(V^\top \tilde{V})} \\ &\stackrel{(\natural)}{\leq} \sqrt{2} \sqrt{1 - \sigma_r^2(V^\top \tilde{V})} = \sqrt{2} \|V^\top \tilde{V}\|_2, \end{aligned}$$

where (\sharp) follows after replacing $V^\top \tilde{V} = U\Sigma W^\top$ in the expression and gathering terms, while (\natural) simply uses the fact that $\sigma_r(V^\top \tilde{V}) \leq 1$ to upper bound the expression inside the square root. Finally, we use the fact that:

$$1 - \sigma_{\min}^2(V^\top \tilde{V}) = \|V_\perp^\top \tilde{V}\|_2^2 = \text{dist}_2^2(V, \tilde{V}).$$

□

Discussion: eigenvalue localization issues. We briefly address the issue of when we can safely assume that the approximate invariant subspace V , utilized in Proposition 3, is the **leading** invariant subspace of the perturbed matrix $A - EV^\top$. While the matrix of Ritz values, S , is within $\sqrt{2} \|E\|_2$ distance of a set of r eigenvalues of A , we do not know whether or not these eigenvalues correspond to the largest (in magnitude) eigenvalues of $A - EV^\top$.

In this case, one has to appeal to algorithm-specific arguments. Recall that A has spectral decomposition $A = V_1 \Lambda_1 V_1^\top + V_2 \Lambda_2 V_2^\top$, where Λ_1 contains the dominant r eigenvalues. Let $V_\perp \in \mathbb{O}_{n, n-r}$ be orthogonal to the approximate eigenvector matrix $V \in \mathbb{O}_{n, r}$. Then the following

$$\begin{bmatrix} V^\top \\ V_\perp^\top \end{bmatrix} (A - EV^\top) \begin{bmatrix} V & V_\perp \end{bmatrix} = \begin{bmatrix} S & V^\top (A - EV^\top) V_\perp \\ V_\perp^\top V S & V_\perp^\top (A - EV^\top) V_\perp \end{bmatrix} = \begin{bmatrix} S & V^\top A V_\perp \\ \mathbf{0} & V_\perp^\top A V_\perp \end{bmatrix}$$

is a Schur decomposition of $A - EV^\top$, with its eigenvalues being the union $S \cup \Lambda(V_\perp^\top A V_\perp)$ – the objective becomes showing that $\|\Lambda(V_\perp^\top A V_\perp)\|_2$ is sufficiently small, after enough progress of the algorithm. By the variational characterization of eigenvalues for symmetric matrices, we

have

$$\lambda_1(V_\perp^\top AV_\perp) = \sup_{x \in \mathbb{S}^{n-1}} |\langle x, V_\perp^\top AV_\perp x \rangle| \quad (31)$$

$$= \sup_{x \in \mathbb{S}^{n-1}} |\langle x, V_\perp^\top V_1 \Lambda_1 V_1^\top V_\perp x \rangle + \langle x, V_\perp^\top V_2 \Lambda_2 V_2^\top V_\perp x \rangle| \quad (32)$$

$$\stackrel{(*)}{\leq} \lambda_1 \|V_\perp^\top V_1\|_2^2 + \lambda_{r+1} \|V_\perp^\top V_2\| \leq 1 \quad (33)$$

Therefore, as soon as $\text{dist}_2(V, V_1) \leq \sqrt{\varepsilon}$, we know that $\Lambda(V_\perp^\top AV_\perp) \leq \lambda_1 \varepsilon + \lambda_{r+1}$; thus when both $\|E\|_2$ and ε are small enough, we can “match” S with the leading invariant subspace of $A - EV^\top$, via the leading eigenvalues of A itself.

References

- Emmanuel Abbe, Jianqing Fan, Kaizheng Wang, and Yiqiao Zhong. Entrywise eigenvector analysis of random matrices with low expected rank. *arXiv e-prints*, art. arXiv:1709.09565, 2017.
- Arash A. Amini, Aiyu Chen, Peter J. Bickel, and Elizaveta Levina. Pseudo-likelihood methods for community detection in large sparse networks. *Ann. Statist.*, 41(4):2097–2122, 08 2013. doi: 10.1214/13-AOS1138.
- Reid Andersen, Fan Chung, and Kevin Lang. Local graph partitioning using pagerank vectors. In *2006 47th Annual IEEE Symposium on Foundations of Computer Science (FOCS’06)*, pages 475–486. IEEE, 2006.
- Mario Arioli, Iain Duff, and Daniel Ruiz. Stopping criteria for iterative solvers. *SIAM Journal on Matrix Analysis and Applications*, 13(1):138–144, 1992.
- Zhaojun Bai, James Demmel, and Alan McKenney. On computing condition numbers for the nonsymmetric eigenproblem. *ACM Transactions on Mathematical Software (TOMS)*, 19(2): 202–223, 1993.
- Mikhail Belkin and Partha Niyogi. Laplacian eigenmaps and spectral techniques for embedding and clustering. In *Advances in neural information processing systems*, pages 585–591, 2002.
- Maria Bennani and Thierry Braconnier. Stopping criteria for eigensolvers. *CERFACS, Toulouse, France, Tech. Rep. TR/PA/94/22*, 1994.
- Austin R Benson, David F Gleich, and Jure Leskovec. Higher-order organization of complex networks. *Science*, 353(6295):163–166, 2016.
- Jeff Bezanson, Alan Edelman, Stefan Karpinski, and Viral B Shah. Julia: A fresh approach to numerical computing. *SIAM review*, 59(1):65–98, 2017.

- Changxiao Cai, Gen Li, Yuejie Chi, H. Vincent Poor, and Yuxin Chen. Subspace Estimation from Unbalanced and Incomplete Data Matrices: $\ell_{2,\infty}$ Statistical Guarantees. *arXiv e-prints*, art. arXiv:1910.04267, Oct 2019.
- Joshua Cape, Minh Tang, and Carey E. Priebe. The two-to-infinity norm and singular subspace geometry with applications to high-dimensional statistics. *Ann. Statist.*, 47(5):2405–2439, 2019. doi: 10.1214/18-AOS1752.
- Yuxin Chen, Chen Cheng, and Jianqing Fan. Asymmetry Helps: Eigenvalue and Eigenvector Analyses of Asymmetrically Perturbed Low-Rank Matrices. *arXiv e-prints*, art. arXiv:1811.12804, Nov 2018.
- Fan R. K. Chung. *Spectral Graph Theory*, volume 92 of *CBMS Regional Conference Series in Mathematics*. American Mathematical Society, 1997.
- Anil Damle and Yuekai Sun. Uniform bounds for invariant subspace perturbations. *arXiv e-prints*, art. arXiv:1905.07865, 2019.
- Anil Damle, Victor Minden, and Lexing Ying. Simple, direct and efficient multi-way spectral clustering. *Information and Inference: A Journal of the IMA*, 8(1):181–203, 06 2018. ISSN 2049-8772. doi: 10.1093/imaiai/iay008.
- James W Demmel. *Applied Numerical Linear Algebra*. Society for Industrial and Applied Mathematics, 1997.
- Justin Eldridge, Mikhail Belkin, and Yusu Wang. Unperturbed: spectral analysis beyond davis-kahan. In Firdaus Janoos, Mehryar Mohri, and Karthik Sridharan, editors, *Proceedings of Algorithmic Learning Theory*, volume 83 of *Proceedings of Machine Learning Research*, pages 321–358. PMLR, 2018. URL <http://proceedings.mlr.press/v83/eldridge18a.html>.
- James P Fairbanks, Anita Zakrzewska, and David A Bader. New stopping criteria for spectral partitioning. In *2016 IEEE/ACM International Conference on Advances in Social Networks Analysis and Mining (ASONAM)*, pages 25–32. IEEE, 2016.
- Jianqing Fan, Kaizheng Wang, Yiqiao Zhong, and Ziwei Zhu. Robust high dimensional factor models with applications to statistical machine learning. *arXiv e-prints*, art. arXiv:1808.03889, Aug 2018.
- Jianqing Fan, Weichen Wang, and Yiqiao Zhong. An ℓ_∞ eigenvector perturbation bound and its application to robust covariance estimation. *Journal of Machine Learning Research*, 18(207): 1–42, 2018. URL <http://jmlr.org/papers/v18/16-140.html>.
- Miroslav Fiedler. Algebraic connectivity of graphs. *Czechoslovak mathematical journal*, 23(2): 298–305, 1973.

- Jerome Friedman, Trevor Hastie, and Robert Tibshirani. *The Elements of Statistical Learning: Data Mining, Inference and Prediction*, volume 1 of *Springer Series in Statistics*. Springer, 2001.
- G. H. Golub and G. Meurant. Matrices, moments and quadrature ii; how to compute the norm of the error in iterative methods. *BIT Numerical Mathematics*, 37(3):687–705, Sep 1997. ISSN 1572-9125. doi: 10.1007/BF02510247.
- Gene H. Golub and Charles F. Van Loan. *Matrix Computations*. Johns Hopkins University Press, 4th ed. edition, 2013.
- Stephen Gower. Netflix prize and svd, 2014.
- N. J. Higham. Matrix nearness problems and applications. In *Proceedings of the IMA Conference on Applications of Matrix Theory*. Oxford University Press, 1988.
- Maurice George Kendall. *Rank correlation methods*. Griffin, 1948.
- Vladimir Koltchinskii and Dong Xia. Perturbation of linear forms of singular vectors under gaussian noise. In Christian Houdré, David M. Mason, Patricia Reynaud-Bouret, and Jan Rosiński, editors, *High Dimensional Probability VII*, pages 397–423, Cham, 2016. Springer International Publishing. ISBN 978-3-319-40519-3.
- RB Lehoucq, DC Sorensen, and C Yang. Arpack users’ guide: Solution of large scale eigenvalue problems with implicitly restarted arnoldi methods. *Software Environ. Tools*, 6, 1997.
- Jure Leskovec, Jon Kleinberg, and Christos Faloutsos. Graphs over time: densification laws, shrinking diameters and possible explanations. In *Proceedings of the eleventh ACM SIGKDD international conference on Knowledge discovery in data mining*, pages 177–187, 2005.
- Jure Leskovec, Kevin J Lang, Anirban Dasgupta, and Michael W Mahoney. Statistical properties of community structure in large social and information networks. In *Proceedings of the 17th international conference on World Wide Web*, pages 695–704, 2008.
- Vince Lyzinski, Daniel L Sussman, Minh Tang, Avanti Athreya, Carey E Priebe, et al. Perfect clustering for stochastic blockmodel graphs via adjacency spectral embedding. *Electronic journal of statistics*, 8(2):2905–2922, 2014.
- Michael W Mahoney, Lorenzo Orecchia, and Nisheeth K Vishnoi. A local spectral method for graphs: With applications to improving graph partitions and exploring data graphs locally. *Journal of Machine Learning Research*, 13(Aug):2339–2365, 2012.
- Lucas Maystre and Matthias Grossglauser. Fast and accurate inference of plackett–luce models. In *Advances in neural information processing systems*, pages 172–180, 2015.
- Francesco Mezzadri. How to generate random matrices from the classical compact groups. *Notices of the AMS*, 54, 2007.

- Eisha Nathan, Geoffrey Sanders, James Fairbanks, Van Emden Henson, and David A. Bader. Graph ranking guarantees for numerical approximations to katz centrality. *Procedia Computer Science*, 108:68 – 78, 2017. doi: <https://doi.org/10.1016/j.procs.2017.05.021>. URL <http://www.sciencedirect.com/science/article/pii/S1877050917305227>. International Conference on Computational Science, ICCS 2017, 12-14 June 2017, Zurich, Switzerland.
- Mark EJ Newman. The mathematics of networks. *The new palgrave encyclopedia of economics*, 2(2008):1–12, 2008.
- B. Parlett. *The Symmetric Eigenvalue Problem*. Classics in Applied Mathematics. Society for Industrial and Applied Mathematics, 1998. doi: 10.1137/1.9781611971163.
- Tai Qin and Karl Rohe. Regularized spectral clustering under the degree-corrected stochastic blockmodel. In *Advances in Neural Information Processing Systems*, pages 3120–3128, 2013.
- Sam T Roweis and Lawrence K Saul. Nonlinear dimensionality reduction by locally linear embedding. *science*, 290(5500):2323–2326, 2000.
- Benedek Rozemberczki, Ryan Davies, Rik Sarkar, and Charles Sutton. Gemsec: Graph embedding with self clustering. In *Proceedings of the 2019 IEEE/ACM International Conference on Advances in Social Networks Analysis and Mining 2019*, pages 65–72. ACM, 2019.
- Yousef Saad. *Numerical Methods for Large Eigenvalue Problems*. Society for Industrial and Applied Mathematics, 2011. doi: 10.1137/1.9781611970739.
- Satu Elisa Schaeffer. Graph clustering. *Computer science review*, 1(1):27–64, 2007.
- G. W. Stewart. Accelerating the orthogonal iteration for the eigenvectors of a hermitian matrix. *Numerische Mathematik*, 13(4):362–376, 1969. ISSN 0945-3245. doi: 10.1007/BF02165413.
- Sebastiano Vigna. Spectral ranking. *Network Science*, 4(4):433–445, November 2016. doi: 10.1017/nws.2016.21. URL <https://doi.org/10.1017/nws.2016.21>.
- Ulrike Von Luxburg. A tutorial on spectral clustering. *Statistics and computing*, 17(4):395–416, 2007.
- Dong Xia and Fan Zhou. The sup-norm perturbation of hosvd and low rank tensor denoising. *Journal of Machine Learning Research*, 20(61):1–42, 2019. URL <http://jmlr.org/papers/v20/17-397.html>.
- Jaewon Yang and Jure Leskovec. Defining and evaluating network communities based on ground-truth. In *2012 IEEE 12th International Conference on Data Mining*, pages 745–754. IEEE, 2012.
- Yilin Zhang and Karl Rohe. Understanding regularized spectral clustering via graph conductance. In *Advances in Neural Information Processing Systems*, pages 10631–10640, 2018.